DOI: https://doi.org/10.54966/jreen.v1i3.1302

Journal of Renewable Energies

Revue des Energies Renouvelables

journal home page: https://revue.cder.dz/index.php/rer

Conference paper

Comparative study of control algorithms MPPT based photovoltaic system with a DC–DC boost converter

Lakhder Ayhar [a,*], **Ahmed Safa** [a], **Abdelmadjid Gouichiche** [a], **Fayssal Elyamani Benmohamed** [b]

[a] *Electrical and Plasma Engineering Laboratory LGEP, Univeristy of Tiaret, Tiaret 14000, Algeria*

[b] *Salhi Ahmed Naama, University Center, Naama 45000, Algeria*

ARTICLE INFO

Article history:

Received September 29, 2024
Accepted October 21, 2024

Keywords:

Sliding mode control,
Fuzzy logic control,
Photovoltaic system,
Maximum power point tracking.

ABSTRACT

Photovoltaic (PV) electricity is a single of more useful forms of clean energy which is seen as being kinder to the environment. The sole drawback of solar photovoltaic (PV) systems is their inefficient energy conversion, which makes it increasingly crucial to extract as much electricity as possible from them. External factors have an impact on the Photovoltaics Current-Voltage (I-V) then and Power-Voltage (P-V) characteristics since they are nonlinear and alter in reaction to temperature and solar light. An electrical circuit known as an MPP tracker (MPPT) is applied to avoid power losses. The literature has a large number of developed and published MPP tracking techniques. Performance comparisons are covered in this study along with the traditional approach (Perturb & Observe) and the more advanced techniques (Fuzzy Logic Control and Sliding Mode Control).

1. INTRODUCTION

A new, less expensive, sustainable energy source with lower carbon emissions is required in light of the most recent alterations to the environment, including climate change, and the sharp rise in the demand for power. In the process of trying to solve the issue, solar energy has produced encouraging outcomes *(Yadav et al. 2012)*. Compared to other forms of energy, because it is clean and environmentally beneficial, one of the newest energy sources, solar energy has a promising future *(Tobon et al. 2017)*. With this energy, electricity can be produced in a variety of ways *(Awan et al. 2022)*, That being said, the most important strategy and the one that drives us in our work depends on the adaptable, trustworthy, and environmentally friendly concept of photovoltaics. Photovoltaic (PV) technology converts a portion of solar radiation into electrical power *(Raza et al. 2019)*. Since this transition produces no noise or gas emissions, it is naturally completely clean *(Loukil et al. 2020)*.

* *Corresponding author, E-mail address: lakhder.ayhar@univ-tiaret.dz*

ISSN: 1112-2242 / EISSN: 2716-8247

The "photovoltaic effect" is a phenomenon that primarily involves solar light transformation into electrical energy using semiconductors called photovoltaic cells. The solar panel, also known as a photovoltaic generator, is made up of a series and parallel arrangement of the necessary number of modules to meet the energy demand must be determined *(Attou et al. 2021)*. On the other hand, temperature and solar radiation substantially affect the PV modules' output voltage, which is one of the primary problems with PV generators. As a result, loads cannot be connected directly to PV modules' output *(Lamzouri et al. 2018)*. Attaining optimal efficiency requires the application of Maximum Power Point Tracking (MPPT) and optimal compatibility between the load and the PV generator. A photovoltaic system can automatically adjust its load to maximize its power output according to the MPPT. In an MPPT system, switch-mode power conversion devices are typically built to connect the load and the PV supply together. By modifying the switching frequency of DC-DC converters, the tracking technique for the correct MPPT is put into practice. This allows the MPP to be tracked by means of a control algorithm that regulates the converter duty cycle *(Attou et al. 2021)*.

A DC-DC converter must be placed between the PV modules and the loads for connection. To optimize the output power utilization of the photovoltaic source, the PV module should operate near its maximum power. Consequently, a control strategy based on an MPPT algorithm can be employed *(Isknan et al. 2023)*.

Numerous strategies and tactics have been put forth to monitor the maximum power produced by photovoltaic panels. The conventional approaches to tracking these trackers, such as hill climbing, in high solar irradiance, perturb and observe and incremental conductance approaches are effective in low solar irradiance, they lose their effectiveness. Neural networks, ant colony optimization, as well as fuzzy logic are instances of artificial intelligence methods that underpin other solutions. These methods greatly increase the system's efficiency, however putting these algorithms into practice requires more coding and computations *(Krachai et al. 2019)*.

These clever strategies could not be sufficiently steady and might be expensive for high levels of uncertainty. When it comes to managing variations in solar radiation for PV system operation, sliding mode control, or SMC, is highly recommended *(Lamzouri et al. 2018)*. Additionally, SMC guarantees load uncertainty and parameter variation stability, robustness, and sensitivity *(Shtessel et al. 2014)*.

Using intelligent controllers like fuzzy logic controllers (FLC) and the conventional P&O technique, the MPPT of a DC boost converter-based photovoltaic system with SMC is reported in this study.

The composition of this document is described below: the mathematical explanation of a photovoltaic panel is covered in section 2, which comes after the introduction. In section 3, discusses MPPT control approaches through an examination of three algorithms: "P&O", "FLC" and "SMC". To assess the offered algorithms and determine which method performs best, the simulation results are analyzed and provided in section 4. We wrap up by drawing a conclusion.

2. SYSTEM OF PHOTOVOLTAIC

Silicon and other semiconductors are used in photovoltaic (solar electric) panels to effectively convert solar radiation into electrical power. The four fundamental parts of a PV systems can be seen in Fig. 1. In the main block, the photovoltaic panel is the power source. The command system, a load, and a static DC-DC converter are located in the second, third, and fourth blocks, respectively *(Isknam et al. 2023)*.

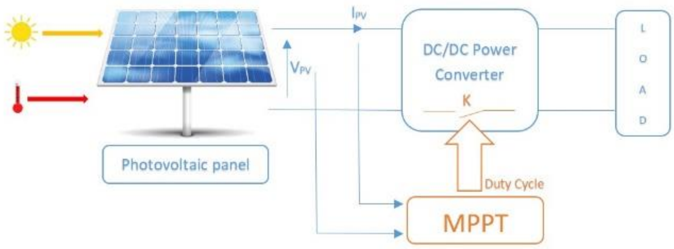

Fig 1. Photographic system block diagram

2.1 Photovoltaic panel

With a photovoltaic (PV) system, sunlight is directly converted to electrical power. A photovoltaic system's primary component is the PV cell. Grouping cells together can create panels or arrays. An array of connected modules delivers the load since it is rare for one module to produce sufficient power for an industrial application. Modules in an array are connected in a manner akin to that of cells inside a module. Furthermore, Modules can be connected in parallel to obtain a higher current or in series to obtain a higher voltage *(Dhar et al. 2012)*.

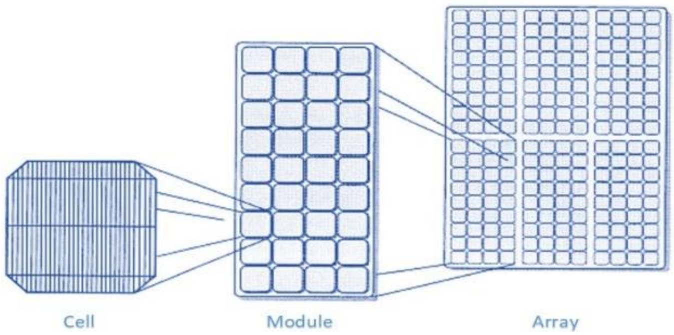

Fig 2. The hierarchy of photovoltaic systems

When PVs are exposed to natural or artificial light, they produce electricity. The operation of a PV cell is demonstrated using a p-n homojunction cell. PV cells consist of a junction formed by two distinct materials, which generates an internal electric field. If photons with power higher than the semiconductor's band gap energy are absorbed, elevation of electrons transition between the valence band and the conduction band. Across the illuminated region of the semiconductor, this operation produces hole-electron pairs. Consequently, these pairs of electrons and holes flow across the junction in opposing directions, creating direct current (DC) power *(Dhar et al. 2012)*.

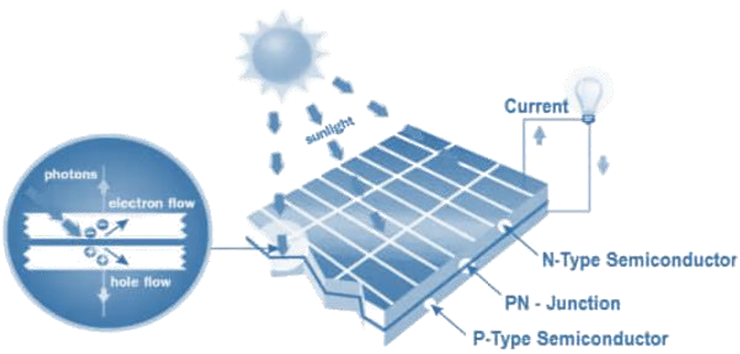

Fig 3. One solar cell diagram

2.2 PV cell modeling and Characteristics

The photovoltaic cell's equivalent circuit Fig. 4 illustrates. The current supply I_{ph} is the photo current of a solar cell. Given that the inherent series and shunt resistors of the cell are R_{sh} and R_s, R_{sh} has a very high value while R_s has a very low value, it is possible to ignore them in order to streamline the analysis. Fig. 5 depicts the PV array equivalent circuit *(Nguyen & Nguyen, 2015),*

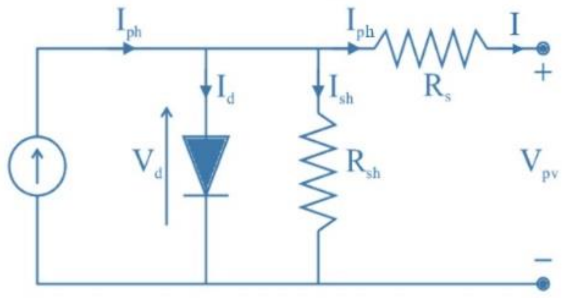

Fig 4. Circuit equivalent to a PV cell

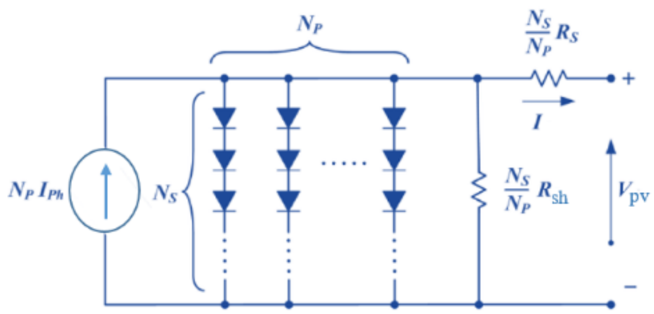

Fig 5. Equivalent circuit of solar array

A solar cell voltage–current characteristic equation is given as:

Module for photocurrent I_{PH}:

$$I_{PH} = [I_{sc} + K_i \times (T - 298{,}15)] \times \frac{G}{1000} \tag{1}$$

Where, I_{ph}: photo current (A); I_{sc}: current during a short circuit (A); K_i: temperature coefficient of current of the cell's short circuit at 25 °C and 1000 W/m^2; T: optimum temperature for operation (K); G: solar radiation (W/m^2).

Reverse saturation of the module's current I_{rs}:

$$I_{rs} = I_{sc} /[\mathrm{e}^{(\frac{qV_{OC}}{N_S knT})} - 1] \tag{2}$$

Here, Ns is the number of cells linked in series; n is the diode ideality factor; k is the Boltzmann constant, which is 1.3805 × 10−23 J/K; q is the charge of an electron, which is equal to 1.6 × 10−19 C; and Voc is the voltage (V) of an open circuit.

The cell temperature, which is established by, determines the current saturation in the module I_0.

$$I_0 = I_{rs} \left[{}^{T}/_{T_r}\right]^3 e^{\left[\frac{q\times E_{g0}}{nk}\left(\frac{1}{T}-\frac{1}{T_r}\right)\right]} \tag{3}$$

In this case, Tr: the designated temperature = 298.15 K; : the band gap energy of the semiconductor, = 1.1 eV; At the moment, the module's PV output is:

$$I = N_p \times I_{PH} - N_p \times I_0 \left[e^{\left(\frac{\frac{V}{N_S}+I\times\frac{R_S}{N_P}}{n\times V_t}\right)} - 1 \right] - I_{sh} \tag{4}$$

With

$$V_t = \frac{k.T}{q} \tag{5}$$

And

$$I_{SH} = \frac{k\times\frac{N_P}{N_S}+I\times R_S}{R_{sh}} \tag{6}$$

The diode's thermal voltage (Vt), the number of parallel PV modules connected, the series resistance (Ω), the shunt resistance (Ω), and Rs are the variables in this instance.

The two main outputs of interest, the I-V and P-V curves, highlight three important features. Upon reaching the P_{max} point, the open circuit voltage (V_{oc}), and the short circuit current (I_{sc}), the output voltage is null. At these points, the panel operates as effectively as possible *(Krachai et al. 2019).*

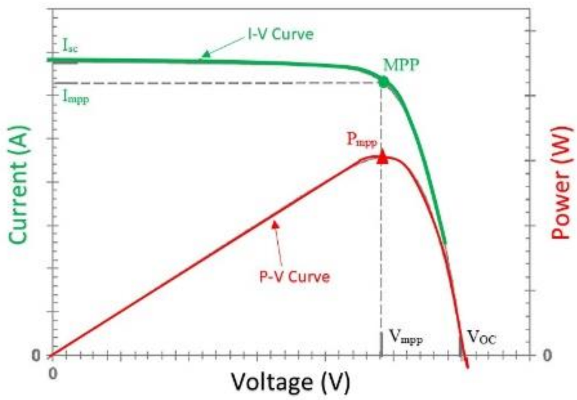

Fig 6. Features of the I-V and P-V curves for a useful photovoltaic device

The PV panel used KC200GT in MATLAB/Simulink with the electrical parameters *(Villalva et al. 2009)* as shown in Table 1.

Fig. 7 demonstrates how the produced current and power output are affected by temperature and irradiance. The maximum power output decreases as the temperature rises because the open-circuit voltage drops. In contrast, a higher irradiance causes the maximum power output and short-circuit current to increase.

Table 1. Details of solar panel specifications for standard test conditions (*STC)

Parameter	Symbol	Value
Maximal Power	P_{max}	200.143 W
Maximum Voltage of Power	V_{mpp}	26.3 V
Maximum Current Power	I_{mpp}	7.6 A
Voltage of Open Circuit	V_{oc}	32.9 V
Current Short Circuit	I_{sc}	8.21 A
Maximum Voltage of the System	-	600 V
Temperature Factor of V_{oc}	K_V	-1.23×10^{-1} V/℃
Temperature Factor of I_{sc}	K_I	3.18×10^{-3} A/℃
Number to each module	N_s	54
Resistance of Shunt	R_{sh}	415.405 Ω
Resistance in Series	R_s	0.221 Ω

*STC: Module temperature of 25°C, AM 1.5 spectrum, and irradiance of 1000W/m^2

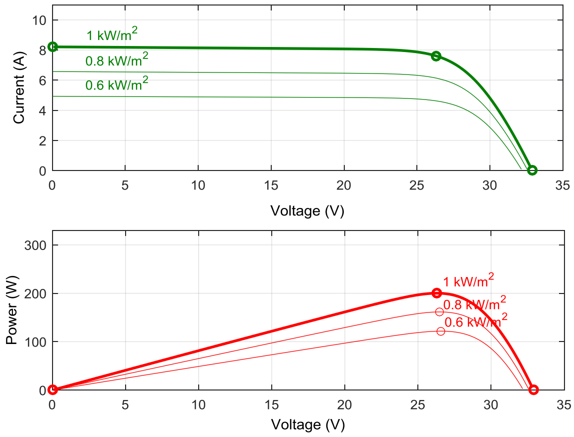

(a)

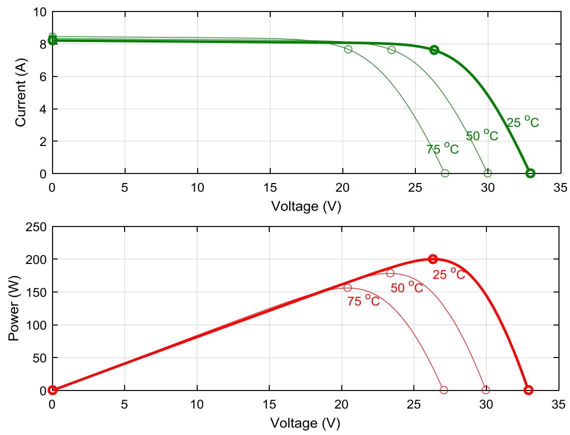

(b)

Fig 7. Temperature (a) and irradiance (b) effects on PV panel properties.

According to the previously mentioned claims, it is essential to keep the panel operating at its maximum power level in spite of variations in temperature and irradiance. Usually, a tool called a maximal power point tracker (MPPT) is used to do this operation.

2.3 DC-DC Power converter

One category of power electronics equipment is a dc-dc converter, known as a chopper occasionally, uses one or more controlled switches to alter a DC voltage source voltage. Due to the low power consumption of essential components including switches, inductors, and capacitors, chopper systems are renowned for their exceptional efficiency *(Abderezak et al. 2015)*.

The ability of an inductor to store energy as a magnetic field is the foundation of the power boost mechanism. Because the output voltage of a step-up converter is based on the duty cycle of the insulated-gate bipolar transistor (IGBT) switch, it is never larger than the supply voltage *(Kumar & Usman, 2018)*.

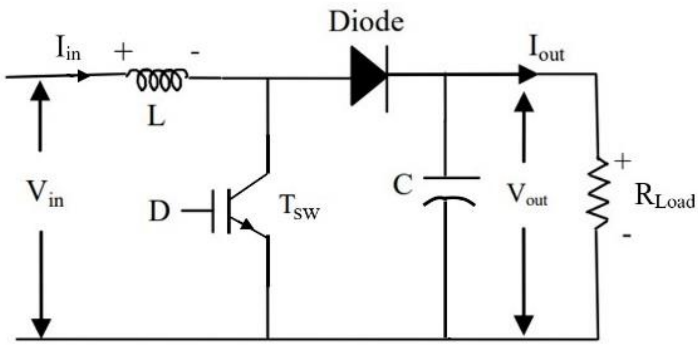

Fig 8. Design circuit for boost converter

When the switch is turned on, magnetic field energy is stored in the inductor. During inductor charging, positive potential is present at the inductor left side terminal. After the switch is opened, with a higher impedance, less current will flow. The inductor's previously generated magnetic field will start to weaken in order to maintain the current flowing toward the load. This will result in the polarity being reversed, making the inductor left side now negative. Since the two sources are in series, Larger voltage applied through diode D will charge the capacitor *Kumar & Usman, 2018; Attou et al. 2021)*.

The following represents the inductor current change rate during turn-on (switch is closed for DT seconds):

$$\frac{di_L}{dt} = \frac{V_{in}}{L} \tag{7}$$

According to Eq. (8), the inductor current change rate during turn-off is as follows: (switch is available for (1 − D)*T seconds)

$$\frac{di_L}{dt} = \frac{V_{in}-V_{out}}{L} \tag{8}$$

For the DC-DC boost converter, the duty ratio D, is as follows:

$$D = 1 - \frac{V_{in}}{V_{out}} \tag{9}$$

It is possible to compute the inductor ripple current Δi_L as follows: (an accurate range for this current is 20% to 40%)

$$\Delta i_L = \frac{V_{in} \times D}{f_s \times L} \tag{10}$$

ΔV_c is voltage ripple, it is 0.1% to 5% of capacitor voltage.

Here is how to find the inductance of an inductor, L:

$$L = \frac{V_{in} \times D}{\Delta i_L \times f_s} \tag{11}$$

The formula yields the capacitance value of capacitor, C:

$$C = \frac{I_{out} \times D}{\Delta V_c \times f_s} \tag{12}$$

where the input voltage is denoted by Vin and the output voltage by Vout. The converter's switching frequency is denoted by fs.

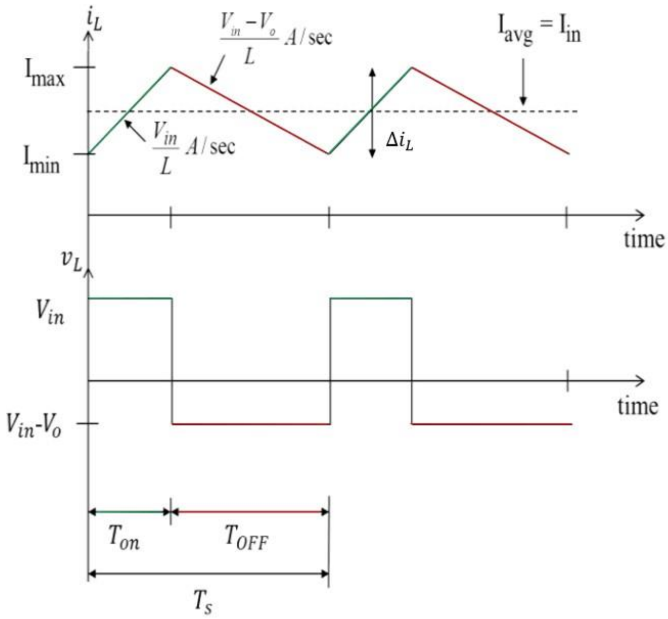

Fig 9. The ideal waveforms for current and voltage

Where I_{max} and I_{min} represent the inductor peak and valley currents, respectively. The quantities v_L and i_L reflect the inductor's current and voltage at any given time, similarly. The average inductor current (I_{avg}) and the input current (I_{in}) are equal. Both the inductor ripple current (ΔI_L) and the load resistor (R_L) are known.

3. MPPT CONTROL ALGORITHM

To ensure that the PV system operates as efficiently as possible, MPPT control is crucial. The idea behind this control is to automatically vary the cycle ratio D until it reaches the ideal value, which will maximize the PV panel power production, hence, the most often used control algorithms will be shown and discussed subsequently. The more well-known PV MPPT algorithms include Open Circuit Voltage, Short Circuit Current, Constant Voltage, Incremental Conductance, and Perturb and Observe, among others.These methods have the benefit of being simple to apply, but they also have disadvantages *(Attou et al. 2021; Abderrezak et al. 2015)*. Additional methods based on distinct concepts include neural circuits, fuzzy control, fractional open circuit voltage or short circuit current, current sweep, and sliding mode controller, among others *(Srisailam & Devadi, 2016)*. These techniques use PV output voltage, output current, or combined to track the MPP. They are predicated on an experimentally derived mathematical link.

3.1 Perturb and Observe (P&O) Method

This technique, referred to as the perturbation and observation technique P&O, is frequently utilized in research MPPT because it is easy to use along with can identify the MPP even in the presence of temperature and light variations. Only the solar panel's voltage and current (V_{PV}, I_{PV}) measurements are needed. The P&O approach, as its name suggests, uses voltage perturbation (V_{PV}) and tracks how this alteration affects the solar panel output power *(Attou et al. 2021; Abderrezak et al. 2015)*.

$P_{pv}(k)$ is computed at each cycle by measuring V_{PV} and IP_V using the P&O method algorithm. The previous value $P_{pv}(k-1)$, which was determined in the previous cycle, is compared to the instantaneous value $P_{pv}(k)$. In case the PV array's output power has risen, P_{pv} is modified similarly to how it was in the preceding cycle.; when it has declined, P_{pv} is modified in the other direction *(Abderrezak et al. 2015)*.

V_{PV} swings around the ideal value $V_{optimum}$ when the MPP is reached. In turn, this oscillation results in a loss of power as it grows with each step of the disturbance, Should this step be large, the MPPT algorithm can react swiftly to abrupt variations in atmospheric conditions. Smaller step increments also result in fewer losses during stable or gradual changes in operating circumstances, but they also make it more difficult for the system to react rapidly to abrupt changes in light or temperature. Based on the needs, an experiment is conducted to find the optimal step increment *(Abderrezak et al. 2015)*.

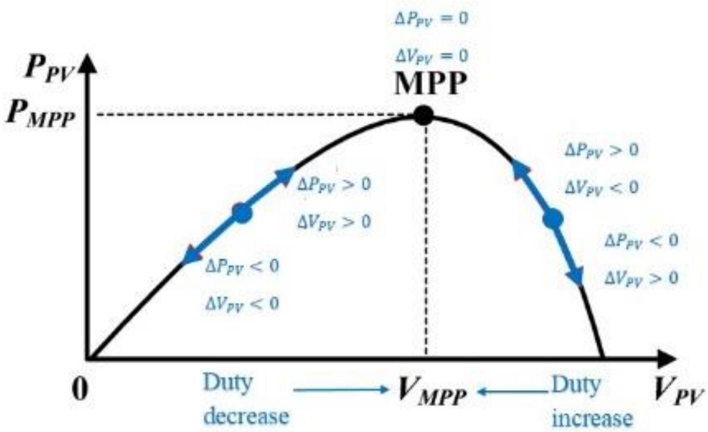

Fig 10. The perturb and observe (P&O) algorithm operating principle

3.2 Fuzzy Logic Control (FLC) Method

Maximum Power Point (MPP) systems are one area where fuzzy logic-based control has recently been applied. Robustness is a benefit of this control mechanism, which does not require exact understanding of the mathematical model of the system. In particular, nonlinear systems are a good fit for this control method. A useful controller for maximizing the power output of PV modules in the face of variable weather is fuzzy logic control, or FLC *(Abderezak et al. 2015; Rastogi et al. 2022)*.

The FLC MPPT maximizes the power production from the PV system by utilizing two inputs and one output. The following defines the output variable, change in duty, and the input parameters, error E and change in error ΔE:

$$E(k) = \frac{\Delta P}{\Delta V} = \frac{P_{pv}(k) - P_{pv}(k-1)}{V_{pv}(k) - V_{pv}(k-1)} \tag{13}$$

$$\Delta E(k) = E(k) - E(k-1) \tag{14}$$

$$\Delta D(k) = D(k) - D(k-1) \tag{15}$$

Where $P_{pv}(k)$ is instantaneous power for PVG, $V_{pv}(k)$ is the equivalent voltage in real time, and k is the sampling time.

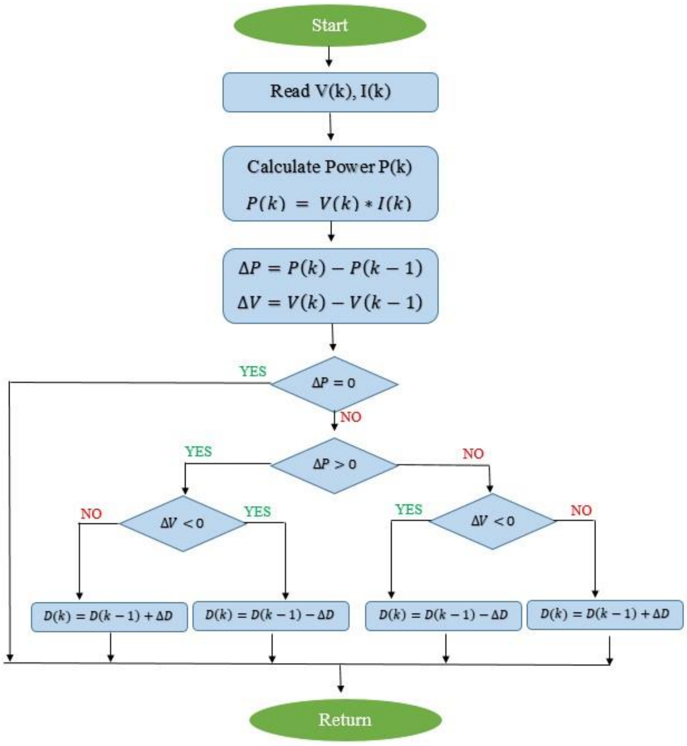

Fig 11. P&O algorithm flowchart

Three processes are involved in the fuzzy logic controllers: fuzzification of crisp input, rule evaluation in the inference engine, and fuzzy output defuzzification from the inference engine *(Rastogi et al. 2022)*.

Crisp input is required for the first category fuzzification process. Using the stored membership function, it transforms the crisp input into fuzzy input. The first step in FLC fuzzification occurs when the fuzzy values are designed *(Rastogi et al. 2022; Narwat & Dhillon, 2021)*.

Rule evaluation is FLC second category. The fuzzy processor, which is part of the rule evaluation process, determines the controlling action that takes place during using the linguistic rules, the response to the set of input values. The outcome of any action produced by the rule evaluation is always ambiguous *(Rastogi et al. 2022; Narwat & Dhillon, 2021)*.

The defuzzification technique is the last category in the fuzzy logic controller procedure. The fuzzy value is transformed into a crisp value during defuzzification *(Rastogi et al. 2022; Narwat & Dhillon, 2021)*.

To achieve an accurate monitoring of the MPP, 25 fuzzy rules were defined for two inputs and one output, symbolized by the membership functions pb: Positive Big, ps: Positive Small, ze: Zero, nb: Negative Big, and ns: Negative Small. For both inputs and outputs, triangle membership functions have been chosen. The fuzzy rules base is similar to that used by *Eltawil & Zhao (2013)*.

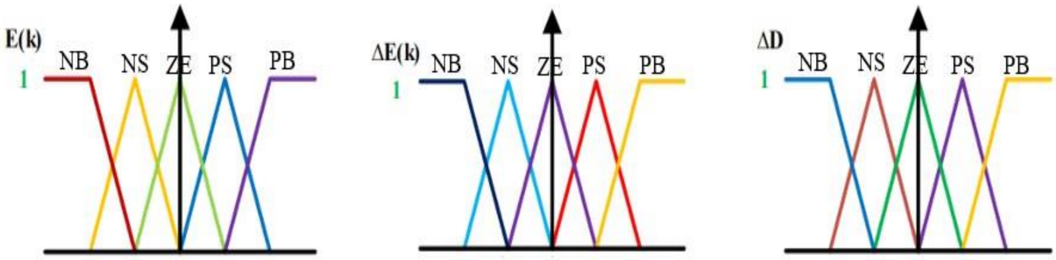

Fig 12. Input, input change, and output membership functions

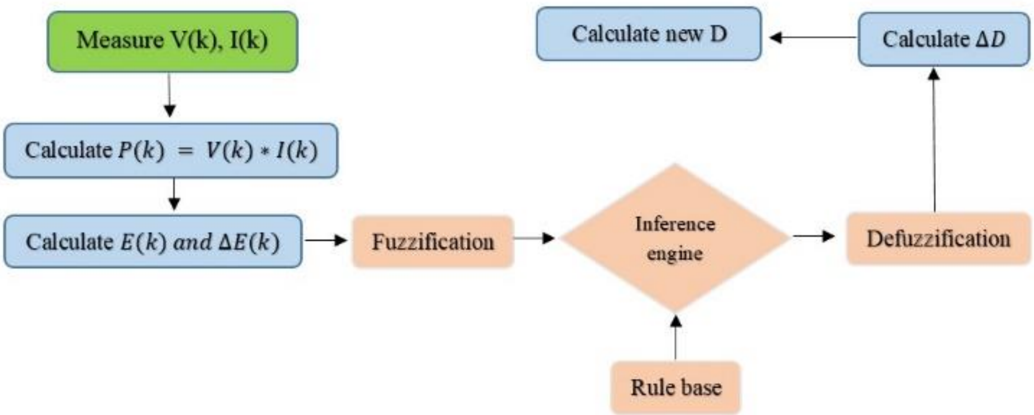

Fig 13. Flowchart of a FLC scheme

Duty cycle is the FLC output that uses a PWM created pulse to drive the DC-DC converter switch.

3.3 Sliding mode controller (SMC) Method

The SMC uses the voltage at the MPP (Vmpp) that was calculated using the P&O method as a guide *(Nelson & Inanç, 2022)*. When the SMC is put into practice, it will generate the control signals required to raise reference voltage to the PV module's output voltage and, eventually, to the MPP *(Nelson & Inanç, 2022; Jain et al. 2020; Safa et al. 2017)*. Considering that the difference between the PV module's reference voltage (Vmpp) and output voltage (Vpv) is the error (e), a sliding surface (s) can be described as follows:

$$s = e = V_{pv} - V_{mpp} \tag{16}$$

The switching law that controls the boost converter is as follows:

$$U = \frac{1}{2}(1 + sign(s)) \tag{17}$$

The position of switching is defined based on the value of s. When s ≥ 0 this happens, the switch will be on; otherwise, it will be off.

Where s is the sliding surface, and is it possible to think of it as

$$s = \frac{dP_{pv}}{dI_{pv}} \tag{18}$$

Where, $P_{pv} = V_{pv} \times I_{pv}$. Therefore, s can be expressed as

$$s = v_{pv} + I_{mpp} \frac{d\, v_{pv}}{d\, I_{mpp}} \tag{19}$$

Where, I_{mpp} represents the MPP current.

After looking at how the position of the operational point and the state of s, It is necessary to choose the following control law:

$$U = \begin{cases} 0\ if\ s \geq 0 \\ 1\ if\ s < 0 \end{cases} \tag{20}$$

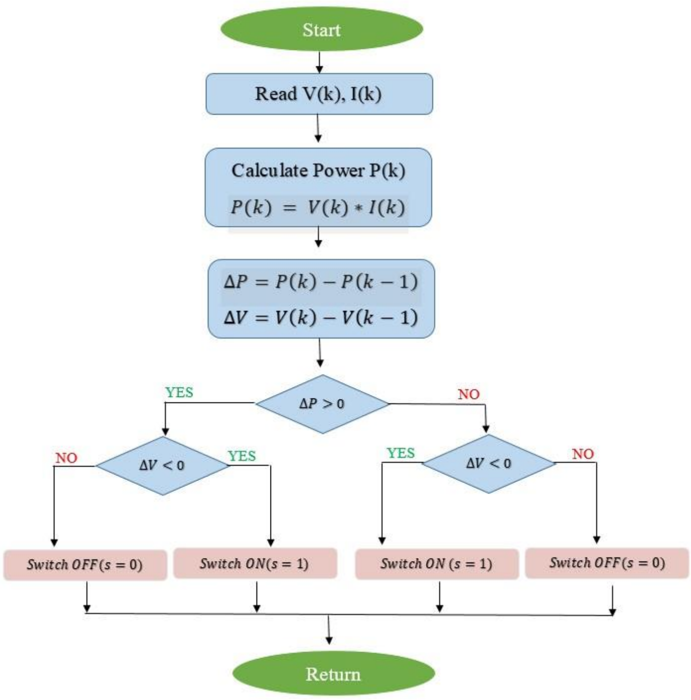

Fig 14. Scheme flowchart for Sliding Mode Controller

4. SIMULATION RESULTS AND DISCUSSION

MATLAB/Simulink software is used to simulate the PV type, which has a controlled DC-DC boost converter, to illustrate the benefits of the sliding mode controller (SMC) based on MPPT algorithms over those of the fuzzy logic controller (FLC) and the traditional P&O MPPT approach at various environmental settings to demonstrate how the SMC and FLC MPPT approach can reliably and efficiently detect the maximum power. The solar panels' properties under typical test parameters are displayed in Table 1. The boost DC-DC converter's data sheet details are shown in Table 3, the simulation model is depicted in Fig. 15. The gating signal that powers the IGBT is produced by the MPPT control block's output.

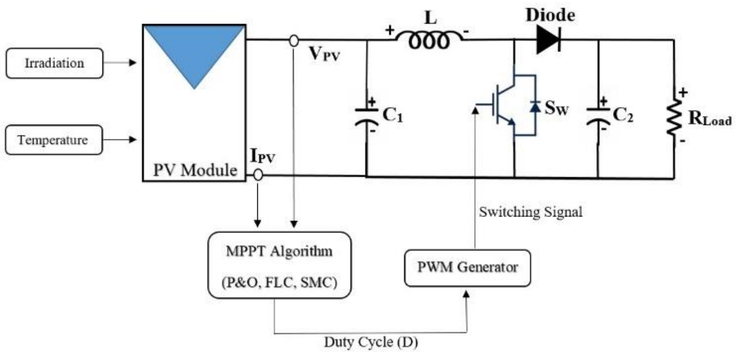

Fig 15. System applied to the simulation model

Table 3. DC-DC boost converter component values

Parameter	Symbol	Value
Capacitance	C_1	1mF
Switching Frequency	f_s	5KHz
Inductance	L	1mH
Capacitance	C_2	1100µF
Resistance	R_{Load}	3.55Ω

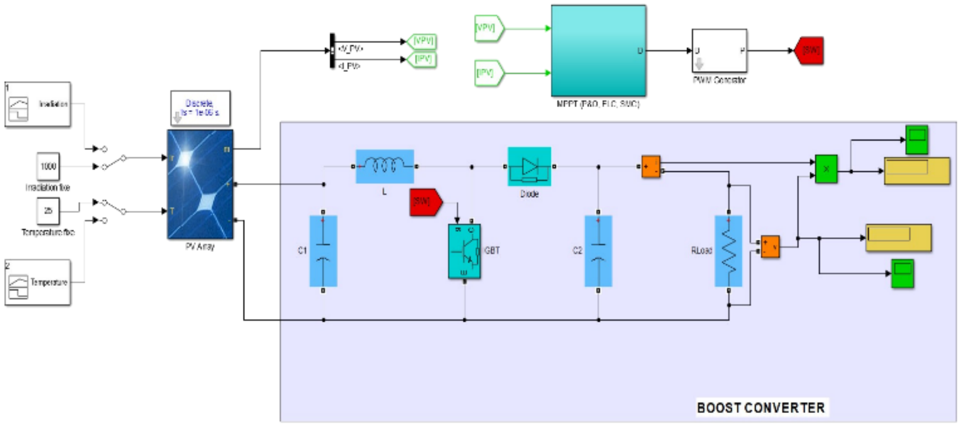

Fig 16. Simulink representation of the photovoltaic system

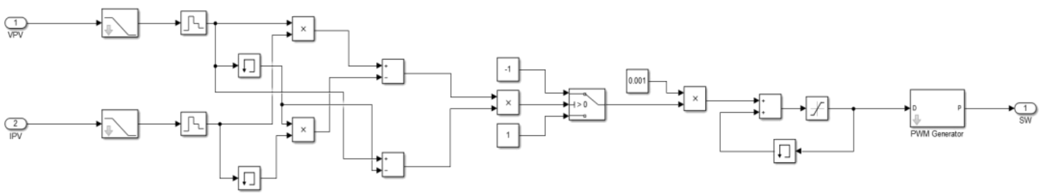

Fig 17. Simulink subsystem of P&O controller

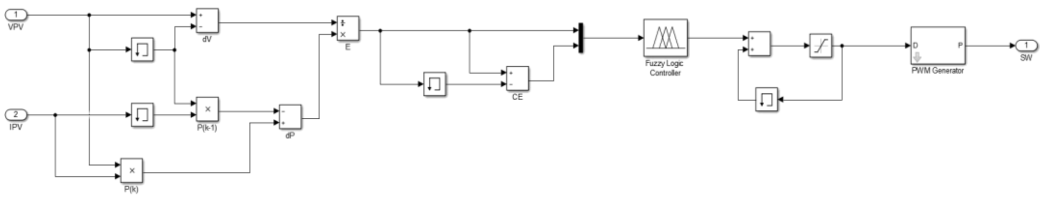

Fig 18. Simulink subsystem of FLC

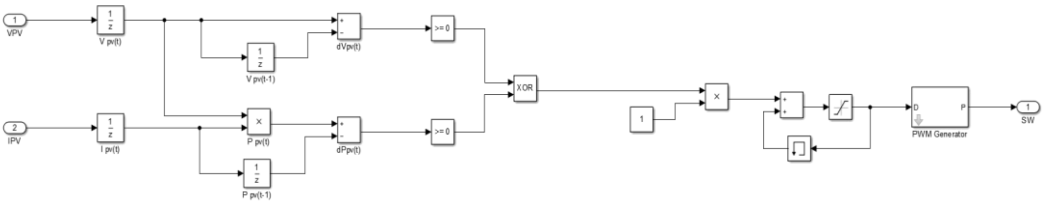

Fig 19. Simulink subsystem of SMC

The purpose of the first test is to confirm that the three techniques can track the MPP at the typical temperature of 25°C and the solar radiation of 1000W/m2. The three controllers' tracked power is shown in Fig. 21.

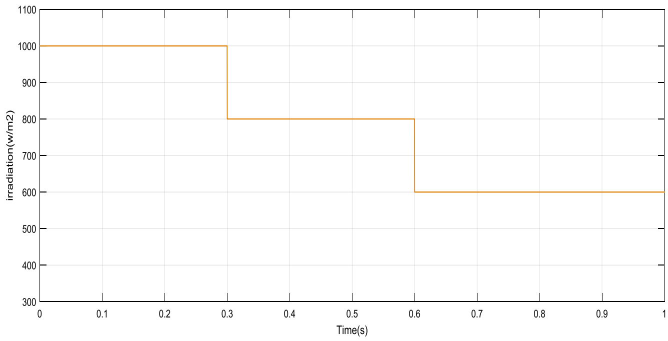

(a)

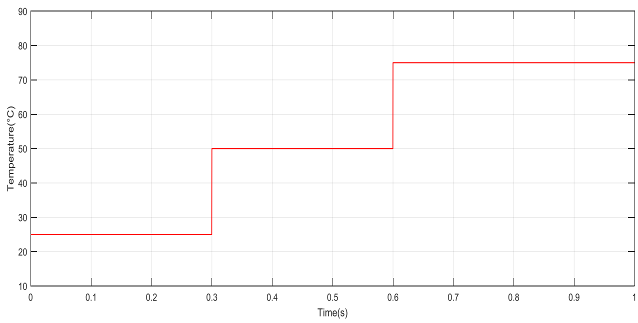

(b)

Fig 20. MATLAB simulation results showing the temperature (b) and radiation (a) profiles that were employed.

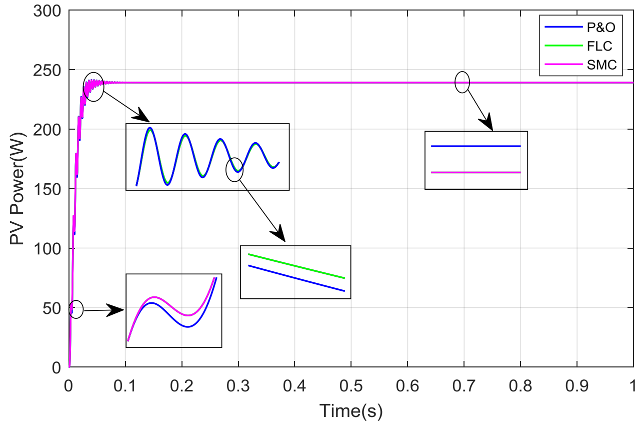

Fig 21. PV power curves produced at 25°C and 1000W/m^2 of solar radiation using the P&O, FLC, and SMC algorithms.

In an additional simulated scenario where there are abrupt changes in solar irradiation levels, 0.3 seconds to get from 1000 W/m2 to 800 W/m2 and 0.6 seconds to go from 800 W/m2 to 600 W/m2 (Fig. 22), it has been noted that the maximum power operating voltage point can be tracked efficiently by P&O, FLC, and SMC algorithms.

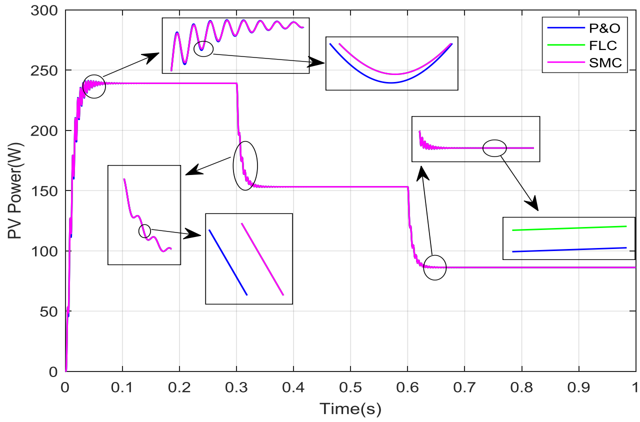

Fig 22. PV power curves produced at 25°C and with varying solar irradiation levels (1000W/m^2, 800W/m^2, and 600W/m^2) using the P&O, FLC, and SMC algorithms

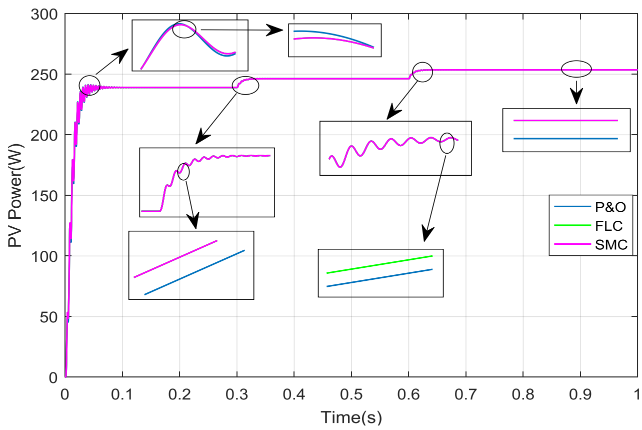

Fig 23. PV power curves produced at 1000W/m^2 of solar radiation and at 25°, 50°, and 75°C temperatures using the P&O, FLC, and SMC algorithms

Fast temperature changes occur in the simulation that follows: 25°C to 50°C in 0.3 seconds and 50°C to 75°C in 0.6 seconds (Fig. 23).

The system known as Maximum Power Point Tracking, or MPPT, which was created utilizing the Sliding Mode Control (SMC) method, has proven to function effectively in a variety of atmospheric situations, as seen by the data shown in Figures 21, 22, and 23. It is evident that the way the Perturb and Observe (P&O) approach responds to sudden variations in light, particularly in the presence of cloud cover, is seriously flawed. In contrast, the fuzzy logic control (FLC) algorithm performs better in terms of adaptability to changing meteorological conditions than the P&O method.

However, we demonstrated how the SMC technique has a minimal tracking error and a good transition response, the FLC algorithm is a more intricate process above SMC and P&O, a reliable and efficient algorithm is the fuzzy logic algorithm. In fact, this algorithm performs better than P&O in terms of response time and operates at the ideal position with less oscillations. It is also distinguished by good behavior in a transient state.

5. CONCUSION

This article presents a thorough overview of the essential elements of a system statement for photovoltaic panels. The KC200GT solar array P-V and I-V properties are examined in detail, and three well-known MPPT algorithms are looked at. In a simulation, the effectiveness of different algorithms is compared to conclude the research. The aim of this research was to maximize a solar generator's output by controlling the duty cycle of boost converter, even with solar insulation and temperature swings present. The FLC algorithm outperforms the P&O methos, based on the simulation findings. Additionally, though the perturb and observe method is commonly employed, the sliding mode controller-based regulation exhibits enhanced behavior and performance compared to other approaches.

REFERENCES

Abderezak, L., Aissa, B. and Hamza, S. (2015). Comparative study of three MPPT algorithms for a photovoltaic system control. World Congress on Information Technology and Computer Applications (WCITCA), Hammamet, Tunisia, 2015, pp. 1-5, doi: 10.1109/WCITCA.2015.7367039.

Attou, A., Fezazi, O. & Mendez, K. (2021). Comparison study of MPPT Algorithms for DC-DC Converter Based PV Systems. 1st International Conference on Sustainable Energy and Advanced Materials. IC-SEAM'21.

Awan, M.M.A., Javed, M.Y., Asghar, A.B. and Ejsmont, K. (2022). Performance optimization of a ten check MPPT algorithm for an off-grid solar photovoltaic system. Energies, 15(16), 2104. doi: 10.3390/en15062104.

Dhar, S., Sridhar, R. and Avasthy, V. (2012). Modeling and Simulation of Photovoltaic Arrays. Department of Electrical & Electronics Engineering, SRM University, Chennai, 2012.

Isknan, I., Asbayou, A., Adaliou, A., Ihlal, A. & Bouhouch, L. (2023). Comparative study and simulation of advanced MPPT control algorithms for a photovoltaic system. Indonesian Journal of Electrical Engineering and Computer Science. 30. 46. 10.11591/ijeecs.v30.i1.

Jain, R.K., Gadiraju, H.K.V, Barry, V.R. and Parne, S.R. (2020). High Performance MPPT Controller based on Adaptive Sliding Mode Control. 2020 21st National Power Systems Conference (NPSC), Gandhinagar, India, 2020, pp. 1-6, doi: 10.1109/NPSC49263.2020.9331826.

Krachai, S., Stambouli, A., Krachai, M. & Bekhti, M. (2019). Experimental investigation of artificial intelligence applied in MPPT techniques. International Journal of Power Electronics and Drive Systems (IJPEDS). 10. 2138. 10.11591/ijpeds.v10.i4.pp2138-2147.

Kumar, S. and Usmam, A. (2018). Effective Design Analysis of a DC-DC Boost Converter with Experimental Validation. International Conference on Computation of Power, Energy, Information and Communication (ICCPEIC), Chennai, India, 2018, pp. 261-268, doi: 10.1109/ICCPEIC.2018.8525165.

Lamzouri, F. -E., Boufounas, E. -M., and El Amrani, A. (2018). A Robust Backstepping Sliding Mode Control for MPPT based Photovoltaic System with a DC-DC Boost Converter. International Conference on Control, Automation and Diagnosis (ICCAD). doi: 10.1109/CADIAG.2018.8751449.

Loukil, K., Abbes, H., Abid, H., Abid, M. and Toumi, A. (2020). Design and implementation of reconfigurable MPPT fuzzy controller for photovoltaic systems. Ain Shams Engineering Journal, 11(12), 319-328. doi: 10.1016/j.asej.2019.10.002.

Narwat, L. & Dhillon, J. (2021). Design and Operation of Fuzzy Logic Based MPPT Controller under Uncertain Condition. Journal of Physics: Conference Series. 1854. 012035. 10.1088/1742-6596/1854/1/012035.

Nelson, M.L. and İnanç, N. (2022). Sliding Mode Control-Based MPPT and Output Voltage Regulation of a Stand-alone PV System. Power Electronics and Drives, 7(1), 159-173. https://doi.org/10.2478/pead-2022-0012.

Nguyen, X. H., & Nguyen, M. P. (2015). Mathematical modeling of photovoltaic cell/module/arrays with tags in Matlab/Simulink. Environmental Systems Research, 4(1). https://doi.org/10.1186/s40068-015-0047-9

Rastogi, D., Jain, M. and Sreejeth, M. (2022). Comparative Study of DC-DC Converters in PV Systems Using Fuzzy Logic MPPT Algorithm. IEEE Delhi Section Conference (DELCON), New Delhi, India, 2022, pp. 1-7, doi: 10.1109/DELCON54057.2022.9753494.

Raza, A., Khan, M.F.N. and Malik, T.N. (2019). Risk constrained energy consumption control for commercial buildings. IEEE 2019 2nd International Conference on Computing, Mathematics and Engineering Technologies. doi: 10.1109/ICOMET.2019.8673458.

Safa, A., Berkouk, E. M., Messlem, Y., et al. (2017). An improved sliding mode controller for a multifunctional photovoltaic grid tied inverter. Journal of Renewable and Sustainable Energy, 9(6).

Shtessel, Y., Edwards, C., Fridman, L. and Levant, A. (2014), Sliding Mode Control and Observation. Control Engineering. https://doi.org/10.1007/978-0-8176-4893-0

Srisailam, S. & Devadi, J. (2016). A Review on Optimization Algorithms for MPPT in Solar PV System under Partially Shaded Conditions.

Tobón, A., Peláez-Restrepo, J., Villegas-Ceballos, J., Serna-Garcés, S., Herrera, J. and Ibeas, A. (2017). Maximum power point tracking of photovoltaic panels by using improved pattern search methods. Energies, 10(19), 1316. doi:10.3390/en10091316.

Villalva, M.G., Gazoli, J.R. and Filho, E.R. (2009). Modeling and circuit-based simulation of photovoltaic arrays. Brazilian Power Electronics Conference, Bonito-Mato Grosso do Sul, Brazil, 1244-1254, doi: 10.1109/COBEP.2009.5347680.

Yadav, A.P.K., Thirumaliah, S., Haritha, G. (2012). Comparison of MPPT Algorithms for DC-DC Converters Based PV Systems, International Journal of Advanced Research in Electrical, Electronics and Instrumentation Engineering 1(1).